

Reduce state of charge estimation errors with an extended Kalman filter algorithm

Anas El Maliki¹, Abdessamad Benlafkih², Kamal Anoune³, Abdelkader Hadjoudja¹

¹Laboratory of Electronic Systems, Information Processing, Mechanics and Energetics, Faculty of Sciences, Ibn-Tofail University, Kenitra, Morocco

²Advanced Systems Engineering Laboratory, National School of Applied Sciences, Ibn-Tofail University, Kenitra, Morocco

³SmartiLAB EMSI-Rabat, Honoris United Universities, Rabat, Morocco

Article Info

Article history:

Received Feb 11, 2023

Revised Jul 28, 2023

Accepted Sep 6, 2023

Keywords:

Energy storage

Equivalent circuit model

Extended Kalman filter

Lithium-ion battery

State of charge estimation

ABSTRACT

Li-ion batteries (LiBs) are accurately estimated under varying operating conditions and external influences using extended Kalman filtering (EKF). Estimating the state of charge (SOC) is essential for enhancing battery efficiency, though complexities and unpredictability present obstacles. To address this issue, the paper proposes a second-order resistance-capacitance (RC) battery model and derives the EKF algorithm from it. The EKF approach is chosen for its ability to handle complex battery behaviors. Through extensive evaluation using a Simulink MATLAB program, the proposed EKF algorithm demonstrates remarkable accuracy and robustness in SOC estimation. The root mean square error (RMSE) analysis shows that SOC estimation errors range from only 0.30% to 2.47%, indicating substantial improvement over conventional methods. These results demonstrate the effectiveness of an EKF-based approach in overcoming external influences and providing precise SOC estimations to optimize battery management. In addition to enhancing battery performance, the results of the study may lead to the development of more reliable energy storage systems in the future. This will contribute to the wider adoption of LiBs in various applications.

This is an open access article under the [CC BY-SA](https://creativecommons.org/licenses/by-sa/4.0/) license.



Corresponding Author:

Anas El Maliki

Laboratory of Electronic Systems, Information Processing, Mechanics and Energetics, Faculty of Sciences, University Ibn Tofail

Kenitra, Morocco

Email: anas.elmaliki@uit.ac.ma

1. INTRODUCTION

Lithium-ion battery (LiB) applications in electric vehicles (EVs) have been growing rapidly [1], and the need for high security and long life is more important than ever before. In aiming to overcome these challenges, considerable effort has been put into providing an advanced battery management system (BMS), which strongly relies upon battery state estimation [2]. Of the four states, the state of charge (SOC) remains critical. However, it is not possible to directly measure the internal SOC. Only measurable signals, such as the battery voltage and the load current, can be used to estimate this value. Therefore, to obtain a precise and stable estimation of SOC, there is a need to set up a formal solution approach to reduce the negative impact of uncertain measurements, such as both current and voltage noise. Any of these common problems can directly impact the effectiveness and efficiency of estimating the SOC. There are three categories of SOC estimation methods: open-circuit voltage (OCV) method, ampere-hour (Ah) method, and model-based methods [3], [4].

As a result of the lack of an adjustment mechanism, the first two approaches are highly prone to uncertainty in the measurements and will unavoidably fail as the measurement errors increase. Conversely, model-based methods generally exhibit improved performance due to the use of a mechanism allowing closed-loop feedback. The main approaches to model the dynamic behaviors of LIBs are the electrochemical model (EM) [5], the equivalent circuit model (ECM) [6], and the data-driven model [7], [8].

The electrochemical model is very precise and capable of describing detailed transport and reaction mechanisms; however, it is challenging to implement in real-time due to the high computation expense. Instead, data-driven models, which include both artificial neural networks and fuzzy logic, tend to be very efficient and do not require consideration of the mechanisms inherent in the process. However, they both demand massive learning inputs, and the overall performance of generalization might not be tuned for the unseen regions of operation. As opposed to the two, the ECM may provide a decent balance of model accuracy and complexity, and as a result, it became the widest-applied model in the BMS.

Several approaches have been proposed to embed into the ECM in order to be able to accurately estimate the SOC. Among them are the extended Kalman filter (EKF) [9], [10], sigma-point Kalman filter (UKF) [11], [12], and cubature Kalman filter (CKF) [13], [14]. Out of these methods, the EKF method is the most widely used due to its high accuracy and efficiency. However, the EKF algorithm's popularity for SOC estimation doesn't negate the fact that its accuracy depends on both the battery model and system noise variable priors [15]. Like other Kalman filters, the EKF relies on statistical models to represent uncertainties in the system. One critical aspect is the specification of noise parameters in the prediction step of the filter. If these noise parameters are not properly estimated or set, the EKF may not accurately account for the uncertainties in the battery behavior, leading to inaccurate SOC predictions [16].

Several research studies have attempted to address the problem of measurement noise by improving the precision of SOC estimations. Sun *et al.* proposed the use of smart adaptive extended Kalman filter (AEKF) [17] and adaptive unscented Kalman filter (AUKF) [18] to estimate battery SOC by considering noise. Maheshwari and Nageswari [19] combined the sunflower optimization algorithm (SFO) with a machine learning model to improve SOC estimation performance using an adaptive Kalman filter, as evidenced by the analysis of the error metric in the estimation results.

This paper first proposes an EKF algorithm that uses an equivalent circuit model, specifically a second-order RC model. The methodology is focused on providing mathematical modeling of the given lithium-ion battery (LiB) and The EKF algorithm. Afterward, these mathematical models are implemented into the developed MATLAB program and then verified in the estimation procedure. Lastly, we set the noise covariance parameters for the SOC estimation algorithm.

An organization for the remaining part of this paper is as outlined here: Section 2 provides an introductory overview of the battery model, parameter identification, and a brief explanation of the EKF algorithm EKF. Section 3 outlines the proposed model's implementation in a MATLAB program. Section 4 validates the proposed model through various simulation results related to the noise covariance parameters. Section 5 summarizes the overall paper.

2. MATHEMATICAL MODELLING OF LIB

2.1. Battery model

A precise assessment of a battery's state of charge requires the use of an appropriate battery model. The ECM [20], [21] is a commonly used model for assessing battery polarization phenomena due to its consideration of electrochemical concentration and polarization. This makes it a convenient method for determining these parameters.

The foundation shown in Figure 1 uses a second-order R_C model to represent a battery's dynamic behavior. This model is critical for understanding the battery's responses to different conditions and inputs. It enables precise study and prediction of battery performance, aiding optimization in various applications.

In this model, a schematic diagram represents internal components, including resistances and capacitors. Internal resistance is marked as R_0 , reflecting inherent resistance within. R_{p1} and R_{p2} denote resistances due to electrochemical and concentration polarizations, depicting how interactions occur with the environment. Lastly, fractional capacitors, C_{p1} and C_{p2} , correspond to electrochemical and concentration polarizations respectively, illustrating energy storage components.

U_{OC} is one of the SOC functions that indicates the voltage across the open circuit in an application. I denotes the total current in a battery pack, essential for assessing its operational state. U_L , U_{p1} , and U_{p2} represent the terminal voltage of the battery pack and the voltages across C_{p1} and C_{p2} respectively, offering insight into the voltage levels in various system components.

It can be shown that Kirchhoff's law is the basis of the circuit equations for this model, and the state space equations that describe this model can be summarized as (1):

$$\begin{cases} U_L = U_{oc} - U_{p1} - U_{p2} - IR_0 \\ \dot{U}_{p1} = -\frac{1}{C_{p1}R_{p1}}U_{p1} + \frac{1}{C_{p1}}I \\ \dot{U}_{p2} = -\frac{1}{C_{p2}R_{p2}}U_{p2} + \frac{1}{C_{p2}}I \end{cases} \quad (1)$$

as a result, the state-space equations can be viewed as a matrix which can be summarized in (2):

$$\begin{cases} \begin{bmatrix} Soc_{k+1} \\ U_{p1,k+1} \\ U_{p2,k+1} \end{bmatrix} = \begin{bmatrix} 1 & 0 & 0 \\ 0 & \alpha_1 & 0 \\ 0 & 0 & \alpha_2 \end{bmatrix} \begin{bmatrix} Soc_k \\ U_{p1,k} \\ U_{p2,k} \end{bmatrix} + \begin{bmatrix} -\Delta t/C_n \\ (1-\alpha_1)R_{p1} \\ (1-\alpha_2)R_{p2} \end{bmatrix} I_k + w_k \\ U_{L,k} = U_{oc}(Soc_k) - U_{p1,k} - U_{p2,k} - I_k R_0 + v_k \end{cases} \quad (2)$$

where $\alpha_i = \exp(-\Delta t/R_{pi}C_{pi})$, Δt denotes the time interval between consecutive measurements. The variables w_k and v_k correspond to noise in the process and the measured noise, respectively.

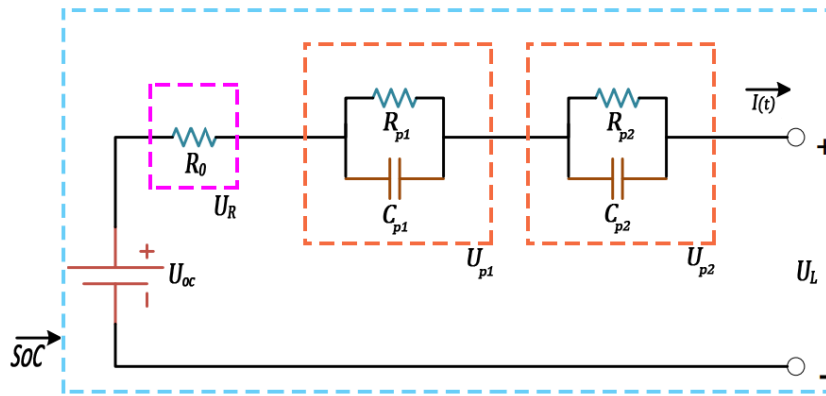


Figure 1. Equivalent circuit model

3. METHOD

3.1. Method process flowchart

According to Figure 2, a proposed model's flow chart is structured in two parts. The first part is a second-order RC model (2RC), which is based on an incoming load current that is used to calculate the SOC. Within the input value, as well as the equation describing the model, we can simulate the terminal battery voltage based on the 2RC model. The last part of the procedure is the EKF estimation. In this step, the EKF algorithm utilizes the voltage values from the 2RC model and the observer battery voltage to estimate the SOC of the battery.

The new European driving cycle (NEDC) [22] is utilized in the proposed model to simulate standard driving conditions. It comprises various driving cycles to mimic typical urban and extra-urban environments in Europe. This standard allows for the consistent comparison of emission levels and fuel consumption between different vehicles.

3.2. Simulation inputs

In accordance with the hybrid pulse power characteristics (HPPC) methodology outlined in 2019 [23], it is established that the relationship between open circuit voltage (OCV) and SOC can be accurately represented using a sixth-order polynomial curve. This polynomial curve serves as a comprehensive model to describe the intricate connection between OCV and SOC, providing a valuable tool for predicting and understanding the battery's behavior across its charge and discharge cycles. Such mathematical representations are crucial in the field of battery management and energy storage system analysis.

$$V_{ocv} = k_0 + k_1 Soc + k_2 Soc^2 + k_3 Soc^3 + k_4 Soc^4 + k_5 Soc^5 + k_6 Soc^6 \quad (3)$$

where, $k_{0\sim 6}$ parameters can be found in Table 1 [24].

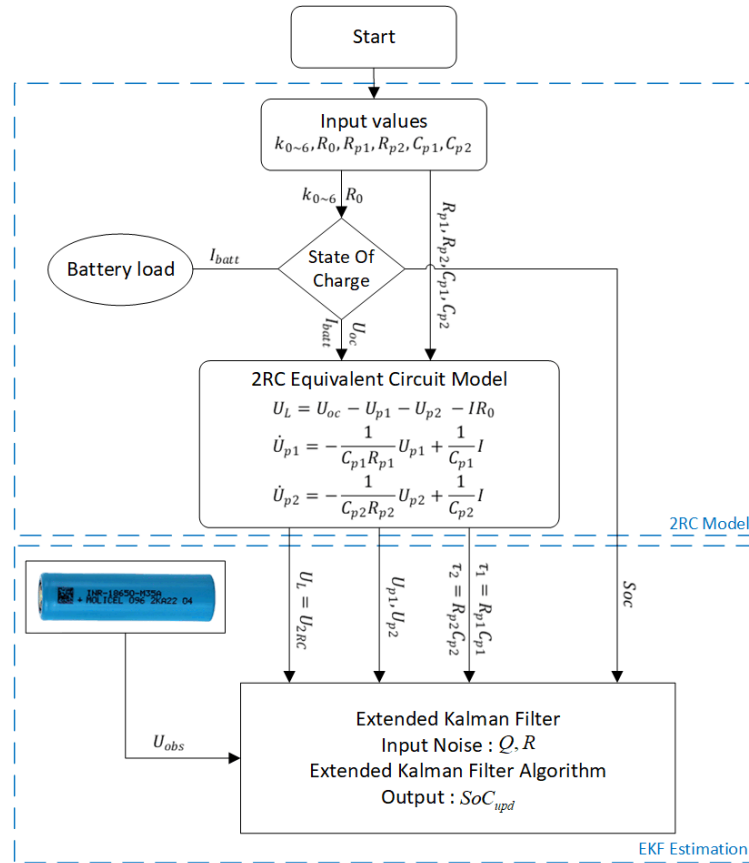


Figure 2. The proposed method flowchart

Table 1. OCV-SOC fitting results at 25 °C

k_0	k_1	k_2	k_3	k_4	k_5	k_6
3.353	2.478	-9.902	19.01	-14.44	2.351	1.319

The proposed model's parameters can be ascertained utilizing the forgetting factor recursive least squares (FFRLS) technique, as illustrated in Table 2 [25]. This method provides an efficient approach to estimate the model parameters iteratively. The FFRLS approach ensures a continuous update of the parameters, making it a robust choice for dynamic systems.

Table 2. Model parameters at 25°C

$R_0(\Omega)$	$R_{p1}(\Omega)$	$C_{p1}(F)$	$R_{p2}(\Omega)$	$C_{p2}(F)$
0.01278	0.00792	524.53	0.05271	4346.76

The 2RC battery model's simulation, using the NEDC as the current profile, is illustrated in Figure 3. Figure 4 presents the terminal voltage estimation based on the key parameters provided in Table 2. Lastly, Figure 5 displays the state of charge estimation, as determined by the empirical model.

The EKF algorithm is applied to our model to estimate the SOC, utilizing the initial covariance matrix defined as (4) as an input parameter. The outcomes of this estimation are illustrated in Figure 6. Figure 7 then portrays the corresponding errors in the SOC, providing a visual representation of the discrepancies in the estimations.

$$P_0 = \begin{bmatrix} 1e^{-1} & 0 & 0 \\ 0 & 1e^{-1} & 0 \\ 0 & 0 & 1e^{-1} \end{bmatrix}, Q = \begin{bmatrix} Qa & 0 & 0 \\ 0 & Qb & 0 \\ 0 & 0 & Qc \end{bmatrix} = \begin{bmatrix} 2e^{-8} & 0 & 0 \\ 0 & 5e^{-3} & 0 \\ 0 & 0 & 3e^{-3} \end{bmatrix}, R = 2e^{-6} \quad (4)$$

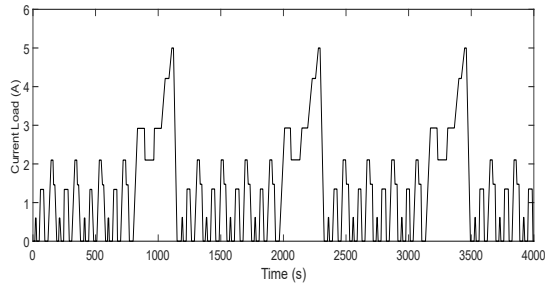


Figure 3. NEDC load current profile

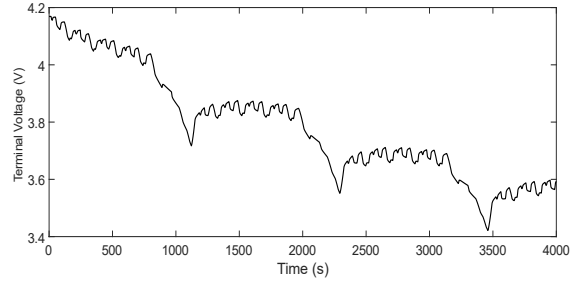


Figure 4. Terminal voltage estimation results

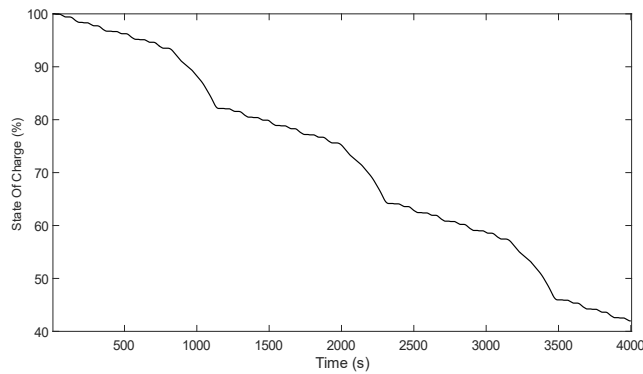


Figure 5. Estimation of SOC using ampere-hour method

Figure 6 illustrates the progression of the state of charge estimation using the EKF compared to the ampere-hour (AH) method. Meanwhile, Figure 7 displays the error over the course of a cycle. From 2,000 seconds onwards, a significant error can be measured in the EKF estimation. Nevertheless, it is important to point out that the maximum drift of the EKF algorithm is 2.3% in comparison to the actual state of charge, which represents a substantial improvement over the AH algorithm.

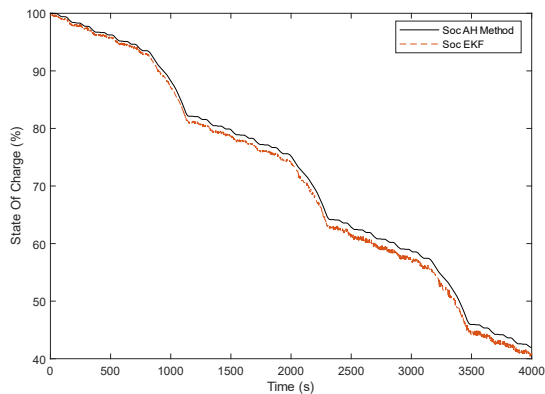


Figure 6. SOC estimated by EKF algorithm

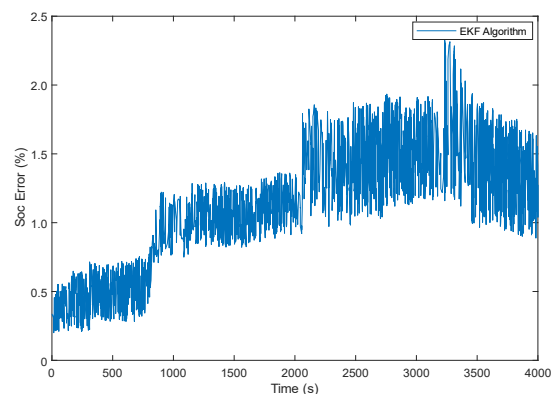


Figure 7. SOC estimated by EKF algorithm

4. RESULTS AND DISCUSSION

To simulate the responses to various input noises related to SOC and process noise (Q) and measurement noise (R), we utilize the EKF algorithm for SOC estimation. Figures 8(a) to (d) illustrate the results of SOC estimation under the new European driving cycle (NEDC) profile, considering varying input noises Q_a , Q_b , Q_c , R, and using the EKF algorithm. The root mean squared errors (RMSEs) of the EKF method are presented in Table 3.

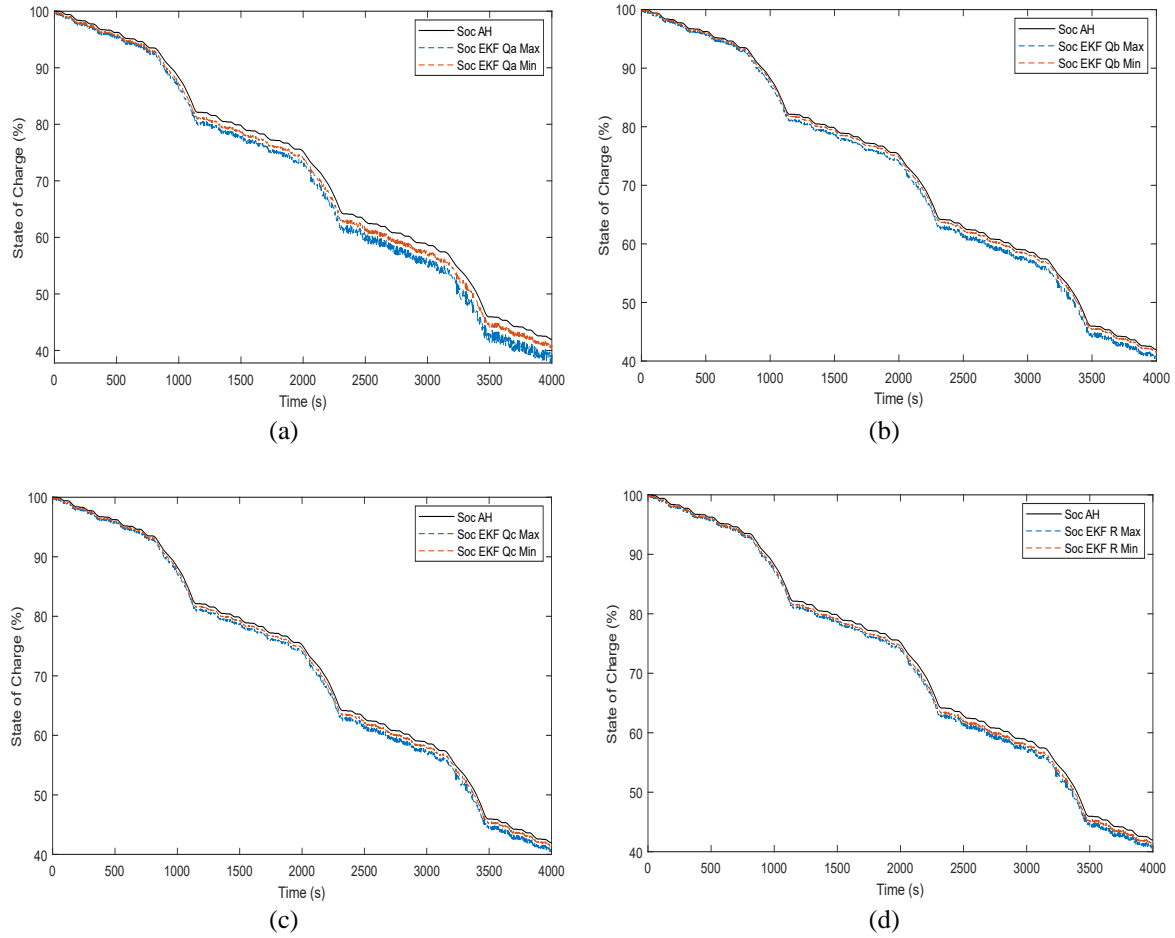


Figure 8. Comparison of SOC estimation under varied noise input (a) Qa, (b) Qb, (c) Qc, and (d) R

Table 3. Estimation of SOC with different noise inputs

Input Noise	Value	Soc (RMSE %)
Qa	$Q_{a \max}$	$2e^{-1}$ 0.0244 (2.44%)
	$Q_{a \min}$	$1e^{-8}$ 0.0117 (1.17%)
Qb	$Q_{b \max}$	$1e^{-3}$ 0.0119 (1.19%)
	$Q_{b \min}$	$5e^{-1}$ 0.0041 (0.41%)
Qc	$Q_{c \max}$	$1e^{-3}$ 0.0118 (1.18%)
	$Q_{c \min}$	$3e^{-1}$ 0.0055 (0.55%)
R	R_{\max}	$1e^{-6}$ 0.0117 (1.17%)
	R_{\min}	$2e^{-1}$ 0.0067 (0.67%)

As shown in Table 3, SOC errors have different scales due to large covariance noise inputs. The proposed approach improves parametric filtering. In this case, the RMSE value for $Q_{a \max}$ is 0.0244, and for $Q_{a \min}$, it is 0.0117, respectively. The SOC curve for these variables as shown in Figure 8(a). Additionally, the RMSE value for $Q_{b \max}$ is 0.0119, and for $Q_{b \min}$, it is 0.0041, respectively. The corresponding SOC curve can be seen in Figure 8(b). The RMSE value for $Q_{c \max}$ is 0.0118, and for $Q_{c \min}$, it is 0.0055, respectively. The SOC curve for these variables can be shown in Figure 8(c). Finally, the RMSE value of R_{\max} is 0.0117, and for R_{\min} , it is 0.0067, respectively. The corresponding SOC curve can be illustrated in Figure 8(d).

Figure 8 and Table 3 reveal a maximum RMSE error of about 2.44% and a minimum of roughly 0.4%. This aligns with Table 3 findings, highlighting the extended Kalman filter's accuracy in estimating the SOC. This accuracy is mainly due to the appropriate input values for its noise covariance.

Table 4 details the EKF estimation boundaries from the parametric study. The RMSE of SOC estimation varies between 2.47% and 0.30% due to different input noise values. Analyzing these variations is crucial for improving SOC estimation accuracy.

Table 4. RMSE of SOC estimation under max and min input noise

Input Noise	Value	Soc (RMSE %)
Max	$Q_{a \max}$	$2e^{-1}$
	$Q_{b \max}$	$1e^{-3}$
	$Q_{c \max}$	$3e^{-3}$
	R_{\max}	$2e^{-6}$
Min	$Q_{a \min}$	$2e^{-8}$
	$Q_{b \min}$	$5e^{-1}$
	$Q_{c \min}$	$3e^{-1}$
	R_{\min}	$2e^{-8}$

Examining Table 4, we observe that the EKF used in the proposed model falls within the range of the min and max values of Q_a , Q_b , Q_c , and R . Based on the subfigure shown in Figure 9, it appears that the optimal EKF estimation error lies between the values of EKF Min and EKF Max. When applying the input noise parameter from Table 4, the curves for SoC EKF, SoC EKF Min, and SoC EKF Max follow the same pattern as shown in Figure 9. Additionally, the RMSE of the SOC estimation varies between 2.47% and 0.30% within the EKF boundaries. The EKF algorithm's optimal key noise values are $Q_{a \min} = 2e^{-8}$, $Q_{b \min} = 5e^{-1}$, $Q_{c \min} = 3e^{-1}$, $R_{\min} = 2e^{-8}$, resulting in 0.30% errors during SOC estimation. Meanwhile, Figure 10 displays the error over the course of a cycle.

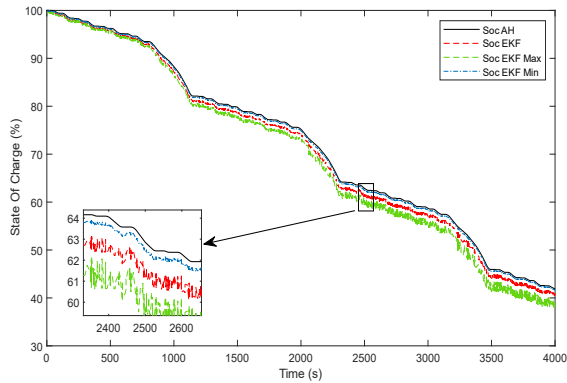


Figure 9. SOC estimation results under maximum and minimum estimation

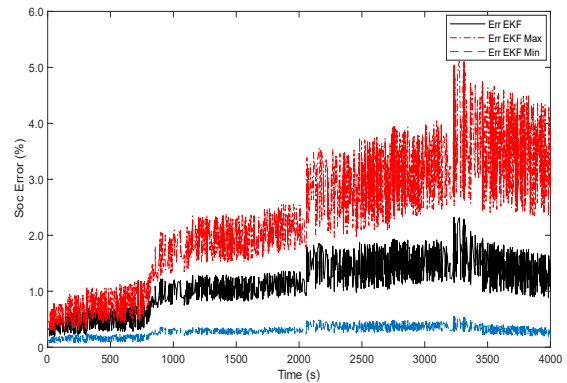


Figure 10. SOC estimation results under maximum and minimum estimation

5. CONCLUSION

This study proposes an EKF method for estimating the SOC of lithium-ion batteries (LiBs) using a second-order RC network. The EKF algorithm is implemented in a MATLAB program developed as part of the project. The mathematical model for the specific LiB is selected and integrated into the program. Subsequently, the battery's behavior is represented using the second-order RC model.

Using different noise covariance matrix values, we simulated and verified our model to ensure its accuracy and robustness. The proposed EKF algorithm demonstrated both accuracy and robustness in the results. The RMSE of the estimated SOC ranged between 2.47% and 0.30%, depending on the studied input noise values. Based on the aforementioned results, we can conclude that the optimal noise covariance matrix values for our algorithm are as follows: $Q_{a \min} = 2e^{-8}$, $Q_{b \min} = 5e^{-1}$, $Q_{c \min} = 3e^{-1}$, $R_{\min} = 2e^{-8}$. Implementing these values will result in an estimation error of 0.30% when using the given algorithm.

REFERENCES

- [1] J. Deng, C. Bae, A. Denlinger, and T. Miller, "Electric vehicles batteries: requirements and challenges," *Joule*, vol. 4, no. 3, pp. 511–515, Mar. 2020, doi: 10.1016/j.joule.2020.01.013.
- [2] X. Hu, F. Feng, K. Liu, L. Zhang, J. Xie, and B. Liu, "State estimation for advanced battery management: key challenges and future trends," *Renewable and Sustainable Energy Reviews*, vol. 114, Oct. 2019, doi: 10.1016/j.rser.2019.109334.
- [3] J. Meng *et al.*, "An overview and comparison of online implementable SOC estimation methods for lithium-ion battery," *IEEE Transactions on Industry Applications*, vol. 54, no. 2, pp. 1583–1591, Mar. 2018, doi: 10.1109/TIA.2017.2775179.
- [4] W. Xu *et al.*, "A novel adaptive dual extended Kalman filtering algorithm for the Li-ion battery state of charge and state of health co-estimation," *International Journal of Energy Research*, vol. 45, no. 10, pp. 14592–14602, Apr. 2021, doi: 10.1002/er.6719.
- [5] J. Shen, Q. Wang, G. Zhao, Z. Ma, and Y. He, "A joint moving horizon strategy for state-of-charge estimation of lithium-ion batteries under combined measurement uncertainty," *Journal of Energy Storage*, vol. 44, Dec. 2021, doi: 10.1016/j.est.2021.103316.

- [6] X. Hu, S. Li, and H. Peng, "A comparative study of equivalent circuit models for Li-ion batteries," *Journal of Power Sources*, vol. 198, pp. 359–367, Jan. 2012, doi: 10.1016/j.jpowsour.2011.10.013.
- [7] M. S. Hossain Lipu *et al.*, "Data-driven state of charge estimation of lithium-ion batteries: algorithms, implementation factors, limitations and future trends," *Journal of Cleaner Production*, vol. 277, Dec. 2020, doi: 10.1016/j.jclepro.2020.124110.
- [8] Y. Boujoudar, H. Elmoussaoui, and T. Lamhamdi, "Lithium-ion batteries modeling and state of charge estimation using artificial neural network," *International Journal of Electrical and Computer Engineering (IJECE)*, vol. 9, no. 5, pp. 3415–3422, Oct. 2019, doi: 10.11591/ijece.v9i5.pp3415-3422.
- [9] G. L. Plett, "Extended Kalman filtering for battery management systems of LiPB-based HEV battery packs - Part 2. Modeling and identification," *Journal of Power Sources*, vol. 134, no. 2, pp. 262–276, Aug. 2004, doi: 10.1016/j.jpowsour.2004.02.032.
- [10] G. L. Plett, "Extended Kalman filtering for battery management systems of LiPB-based HEV battery packs - Part 3. State and parameter estimation," *Journal of Power Sources*, vol. 134, no. 2, pp. 277–292, Aug. 2004, doi: 10.1016/j.jpowsour.2004.02.033.
- [11] G. L. Plett, "Sigma-point Kalman filtering for battery management systems of LiPB-based HEV battery packs. Part 1: Introduction and state estimation," *Journal of Power Sources*, vol. 161, no. 2, pp. 1356–1368, Oct. 2006, doi: 10.1016/j.jpowsour.2006.06.003.
- [12] G. L. Plett, "Sigma-point Kalman filtering for battery management systems of LiPB-based HEV battery packs. Part 2: Simultaneous state and parameter estimation," *Journal of Power Sources*, vol. 161, no. 2, pp. 1369–1384, Oct. 2006, doi: 10.1016/j.jpowsour.2006.06.004.
- [13] J. Luo, J. Peng, and H. He, "Lithium-ion battery SOC estimation study based on Cubature Kalman filter," *Energy Procedia*, vol. 158, pp. 3421–3426, Feb. 2019, doi: 10.1016/j.egypro.2019.01.933.
- [14] I. Arasaratnam and S. Haykin, "Cubature kalman filters," *IEEE Transactions on Automatic Control*, vol. 54, no. 6, pp. 1254–1269, Jun. 2009, doi: 10.1109/TAC.2009.2019800.
- [15] C. Huang, Z. Wang, Z. Zhao, L. Wang, C. S. Lai, and D. Wang, "Robustness evaluation of extended and unscented Kalman filter for battery state of charge estimation," *IEEE Access*, vol. 6, pp. 27617–27628, 2018, doi: 10.1109/ACCESS.2018.2833858.
- [16] R. Xiong, J. Cao, Q. Yu, H. He, and F. Sun, "Critical review on the battery state of charge estimation methods for electric vehicles," *IEEE Access*, vol. 6, pp. 1832–1843, 2017, doi: 10.1109/ACCESS.2017.2780258.
- [17] D. Sun *et al.*, "State of charge estimation for lithium-ion battery based on an intelligent adaptive extended Kalman filter with improved noise estimator," *Energy*, vol. 214, Jan. 2021, doi: 10.1016/j.energy.2020.119025.
- [18] D. Sun, X. Yu, C. Zhang, C. Wang, and R. Huang, "State of charge estimation for lithium-ion battery based on an intelligent adaptive unscented Kalman filter," *International Journal of Energy Research*, vol. 44, no. 14, pp. 11199–11218, 2020, doi: 10.1002/er.5690.
- [19] A. Maheshwari and S. Nageswari, "Real-time state of charge estimation for electric vehicle power batteries using optimized filter," *Energy*, vol. 254, Sep. 2022, doi: 10.1016/j.energy.2022.124328.
- [20] M.-K. Tran, A. Mevawala, S. Panchal, K. Raahemifar, M. Fowler, and R. Fraser, "Effect of integrating the hysteresis component to the equivalent circuit model of Lithium-ion battery for dynamic and non-dynamic applications," *Journal of Energy Storage*, vol. 32, Dec. 2020, doi: 10.1016/j.est.2020.101785.
- [21] X. Lai, Y. Zheng, and T. Sun, "A comparative study of different equivalent circuit models for estimating state-of-charge of lithium-ion batteries," *Electrochimica Acta*, vol. 259, pp. 566–577, Jan. 2018, doi: 10.1016/j.electacta.2017.10.153.
- [22] H. Jbari, R. Askour, and B. B. Idrissi, "Fuzzy logic-based energy management strategy on dual-source hybridization for a pure electric vehicle," *International Journal of Electrical and Computer Engineering*, vol. 12, no. 5, pp. 4903–4914, Oct. 2022, doi: 10.11591/ijece.v12i5.pp4903-4914.
- [23] J. Peng, J. Luo, H. He, and B. Lu, "An improved state of charge estimation method based on cubature Kalman filter for lithium-ion batteries," *Applied Energy*, vol. 253, Nov. 2019, doi: 10.1016/j.apenergy.2019.113520.
- [24] Z. He *et al.*, "State-of-charge estimation of lithium ion batteries based on adaptive iterative extended Kalman filter," *Journal of Energy Storage*, vol. 39, Jul. 2021, doi: 10.1016/j.est.2021.102593.
- [25] Z. Zhang, L. Jiang, L. Zhang, and C. Huang, "State-of-charge estimation of lithium-ion battery pack by using an adaptive extended Kalman filter for electric vehicles," *Journal of Energy Storage*, vol. 37, May 2021, doi: 10.1016/j.est.2021.102457.

BIOGRAPHIES OF AUTHORS



Anas El Maliki    received a B.S degree in fundamental physics studies from Mohammed V University of Rabat, in 2014 and an M.S. degree in physics and new technology from Hassan II University of Casablanca, in 2017. Currently working toward a Ph.D. degree in energy storage and sustainable energy at Ibn Tofail University Kenitra. He can be contacted at email: anas.elmaliki@uit.ac.ma.



Abdessamad Benlafkih    received the B.S. and M.S. degrees, from the University of Sciences Dhar El Mehraz Fez, In 1997 and 2003, respectively. And the Ph.D. degree in electrical engineering from the University Ibn Tofail Kenitra in 2015. He was a teacher in the secondary cycle from 2004 to 2020. And in 2020, He has been a professor of electrical power engineering at University Ibn Tofail Kenitra Morocco. He can be contacted at email: abdessamad.benlafkih@uit.ac.ma.



Kamal Anoune     currently a research professor at EMSI-Rabat, Honoris United Universities, he received his state engineering degree in electrical engineering in 2012, after he launched his start-up specializing in automation and renewable energy, his passion for knowledge in R&D led him to rejoin university in 2015 and obtained his Ph.D. degree in 2020 related to sizing-optimization of PV-wind-battery based micro-grid system, his current works are focused in smart grid, energy auditing, green hydrogen, and energy management opportunities. He can be contacted at email: kamal.anoune@gmail.com.



Abdelkader Hadjoudja     was an engineer and was awarded a doctorate in Microelectronics by the National Polytechnic Institute of Grenoble, France, in 1997. He worked for 6 years as PLD Leader Engineer Software in Atmel, Grenoble, France, and as a consultant within design and reuse. Since July 2010, he became a full professor of electronics at Ibn Tofail University Kenitra. He can be contacted at email: abdelkader.hadjoudja@uit.ac.ma.